

# Selectivity and Directed Charge Transfer through an Electroactive Metallopolymer Film

Charles D. Ellis, W. Rorer Murphy, Jr., and Thomas J. Meyer\*

Contribution from the Department of Chemistry, University of North Carolina, Chapel Hill, North Carolina 27514. Received April 10, 1981. Revised Manuscript Received May 28, 1981

**Abstract:** The voltammetric properties of the couples  $\text{Ru}(\text{bpy})_2(\text{py})\text{Cl}^{2+/+}$  and  $\text{Fe}(\eta^5\text{-C}_5\text{H}_5)_2^{+/0}$  in acetonitrile have been investigated at Pt electrodes which have been chemically modified by electropolymerization of  $\text{Ru}(\text{bpy})_2(\text{vpy})_2^{2+}$  (bpy is 2,2'-bipyridine; vpy is 4-vinylpyridine). For the metal complex sites in the polymer, in addition to Ru(III)/Ru(II) and ligand-based reduction waves, both oxidative and reductive prewaves are observed. At low surface coverages of electropolymerized  $\text{Ru}(\text{bpy})_2(\text{vpy})_2^{2+}$ , the wave for the  $\text{Ru}(\text{bpy})_2(\text{py})\text{Cl}^{2+/+}$  couple in the external solution is diffusional in character. However, at higher surface coverages the contribution from the diffusional wave becomes distorted and decreases to be replaced by an oxidative spike which appears to be triggered by the oxidative prewave. The two different types of waves show the existence of two different pathways for charge transfer through the film to the electrode. The same effect is observed for the  $\text{Fe}(\eta^5\text{-C}_5\text{H}_5)_2^{+/0}$  couple but the oxidative spike appears only at higher surface coverages. In the presence of both  $\text{Ru}(\text{bpy})_2(\text{py})\text{Cl}^+$  and  $\text{Fe}(\eta^5\text{-C}_5\text{H}_5)_2$ , the diffusional pathway for the ruthenium complex is blocked which provides a basis for the selective oxidation of  $\text{Fe}(\eta^5\text{-C}_5\text{H}_5)_2$  in the presence of  $\text{Ru}(\text{bpy})_2(\text{py})\text{Cl}^+$ . At high surface coverages, the sole charge-transfer pathway is through the oxidative spike. The net effect is to achieve directed electron transfer from the solution to the electrode since  $\text{Ru}^{\text{III}}(\text{bpy})_2(\text{py})\text{Cl}^{2+}$  does not undergo re-reduction at the electrode until the onset of  $\text{bpy}/\text{bpy}^\cdot$  reduction at  $E \leq -1.1$  V.

In a recent paper, the preparation of thin films of 2,2'-bipyridine (bpy) complexes of iron and ruthenium on platinum, glassy carbon,  $\text{SnO}_2$ , and  $\text{TiO}_2$  electrodes was described.<sup>1</sup> The films were prepared by reductive electropolymerization of complexes containing as ligands 4-vinylpyridine ( $\text{CCNCCCCH}=\text{CH}_2$ , vpy) or 4-methyl-4'-vinyl-2,2'-bipyridine. With use of this technique, bilayer films can be prepared such that complexes having different Ru(III)/Ru(II) redox potentials are present in spatially segregated layers. The resulting bilayer films constitute a rectifying interface, and directed charge transfer from the outside film to the electrode has been observed.<sup>1</sup> Directed charge transfer from a molecule dissolved in solution through a film on an electrode has been observed by Anson and Oyama in the electrochemical oxidation of Fe(II) to Fe(III) mediated by ionically bound  $\text{IrCl}_6^{2-}$  in a protonated poly(4-vinylpyridine) film.<sup>2</sup>

One of the advantages of the preparation of films by electropolymerization is that film thickness can be systematically and reproducibly varied.<sup>1,3</sup> Some of the variables that control film thickness are monomer concentration and the number of reductive scans through the  $\text{bpy}/\text{bpy}^\cdot$  region, where electropolymerization is initiated. We have taken advantage of our ability to make systematic variations in polymer films to study how the electrochemical characteristics of external redox couples in solution vary with film thickness. Our experiments have led to some remarkable observations whose origins lie in the ability of the polymer film to act as a mediator between the electrode and the external solution.

## Experimental Section

All experiments were performed in acetonitrile with 0.1 M tetraethylammonium perchlorate (TEAP) as supporting electrolyte. TEAP was prepared using a previously published technique.<sup>4</sup> The electrolyte was purified by recrystallization from hot water four times, dried under vacuum at 100 °C for ca. 10 h, and stored in a vacuum desiccator. Acetonitrile (Burdick and Jackson) was used as received. The complexes  $[\text{Ru}(\text{bpy})_2(\text{py})\text{Cl}](\text{PF}_6)$  and  $[\text{Ru}(\text{bpy})_2(\text{vpy})_2](\text{PF}_6)_2$  were synthesized as previously reported.<sup>1</sup>

Electrochemical measurements were recorded versus the saturated sodium chloride calomel electrode (SSCE, +0.236 V N.H.E.<sup>5</sup>) at ca. 23

°C (room temperature) and are uncorrected for junction potential effects. The electropolymerizations were carried out in three-compartment "H" cells of conventional design. Most of the electrochemical measurements were performed in two-compartment cells utilizing a Luggin probe for the reference electrode to minimize IR drop. No external IR compensation was employed. Cyclic voltammograms were obtained using a Princeton Applied Research Model 175 universal programmer and Model 173 potentiostat. The voltammograms were recorded on either a Hewlett-Packard 7015B X-Y recorder or a Tektronix 564B storage oscilloscope. The electrodes used were platinum disks silver-soldered onto brass mounts and press-fitted into Teflon shrouds. The platinum surfaces were pretreated by polishing with 1  $\mu\text{m}$  diamond paste (Buehler) on a Gould 550/140 rpm polishing wheel (Buehler). Solutions were degassed for ca. 20 min with a solvent-saturated argon stream. Trace oxygen and water were removed by passing the argon through a column packed with R3-11 catalyst (Chemical Dynamics Corp.), a column packed with potassium hydroxide, and finally a column packed with 4 Å molecular sieves (Davidson).

Surface coverages in  $\text{mol}/\text{cm}^2$  were evaluated by graphical integration of the areas under the cyclic voltammetric wave for the Ru(III)/Ru(II) reduction using a Keuffel and Esser No. 620000 polar planimeter.<sup>6</sup> Estimates of the number of "layers" were based on a hard-sphere model using a radius of 7.4 Å for the electropolymerized  $[\text{Ru}(\text{bpy})_2(\text{vpy})_2](\text{PF}_6)_2$  sites.<sup>7</sup> However, it is doubtful that polymer growth actually occurs in regular layers and complete coverage of the surface requires many "layers", as the results of this paper show.

**Electropolymerization.** The electropolymerization of a  $5 \times 10^{-3}$  M solution of  $[\text{Ru}(\text{bpy})_2(\text{vpy})_2](\text{PF}_6)_2$  in acetonitrile that contains 0.1 M TEAP as supporting electrolyte was initiated by cyclic voltammetric scans in a potential region (-1.0 to -1.5 V) which results in the reduction of a  $\pi^*$  molecular orbital of the bipyridine ligand. This reduction presumably initiates a free-radical, anionic polymerization pathway, leading to a polymer film on the electrode surface which exhibits the linear  $i_p$  vs.  $\nu$  (scan rate) dependence diagnostic of a surface-confined process.<sup>8</sup> As discussed elsewhere,<sup>9</sup> the thickness of the films can be systematically and reproducibly varied. Surface coverage per reductive scan increases with increasing monomer concentration and if the reductive scan is extended through both bpy reduction waves instead of only the first.

## Results

The cyclic voltammogram of a platinum electrode covered by a film of electropolymerized *cis*- $\text{Ru}(\text{bpy})_2(\text{vpy})_2^{2+}$  in acetonitrile (0.1 M TEAP) is shown in Figure 1. In addition to the Ru-

(1) Abruña, H. D.; Denisevich, P.; Umaña, M.; Meyer, T. J.; Murray, R. W. *J. Am. Chem. Soc.* **1981**, *103*, 1.

(2) Oyama, N.; Anson, F. C. *Anal. Chem.* **1980**, *52*, 1192-1198.

(3) Abruña, H. D., Ph.D. Dissertation, University of North Carolina, Chapel Hill, N.C., 1980.

(4) Sawyer, D. T.; Roberts, J. L. "Experimental Electrochemistry for Chemists"; Wiley-Interscience: New York, 1974; p 212.

(5) Bard, A. J.; Faulkner, L. R. "Electrochemical Methods"; John Wiley and Sons, Inc.: New York, 1980; end pages.

(6) Oyama, N.; Anson, F. C. *J. Electrochem. Soc.* **1980**, *127*, 640-647. Anson and Oyama note that in some cases not all of the immobilized complex is oxidized or reduced during the course of a cyclic voltammogram, so our values may only be lower limits.

(7) Murray, R. W. *Acc. Chem. Res.* **1980**, *13*, 135.

(8) Bard, A. J.; Faulkner, L. R. *Acc. Chem. Res.* **1980**, *13*, 522.

(9) Denisevich, P.; Abruña, H. D.; Leidner, C. R.; Meyer, T. J.; Murray, R. W. *Inorg. Chem.*, in press.

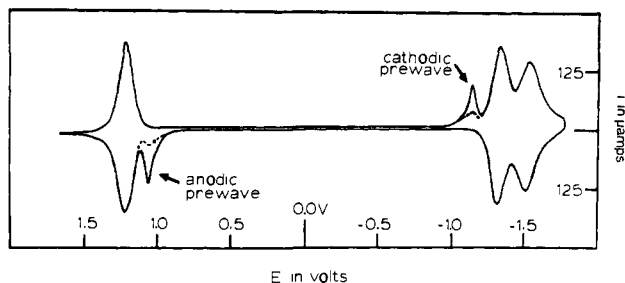


**Figure 1.** Cyclic voltammogram of a platinum electrode coated with  $9.1 \times 10^{-10}$  mol/cm<sup>2</sup> (ca. 9.4 monolayers)<sup>7</sup> of electropolymerized Ru(bpy)<sub>2</sub>(vpy)<sub>2</sub><sup>2+</sup>. The scan rate is 200 mV/s.

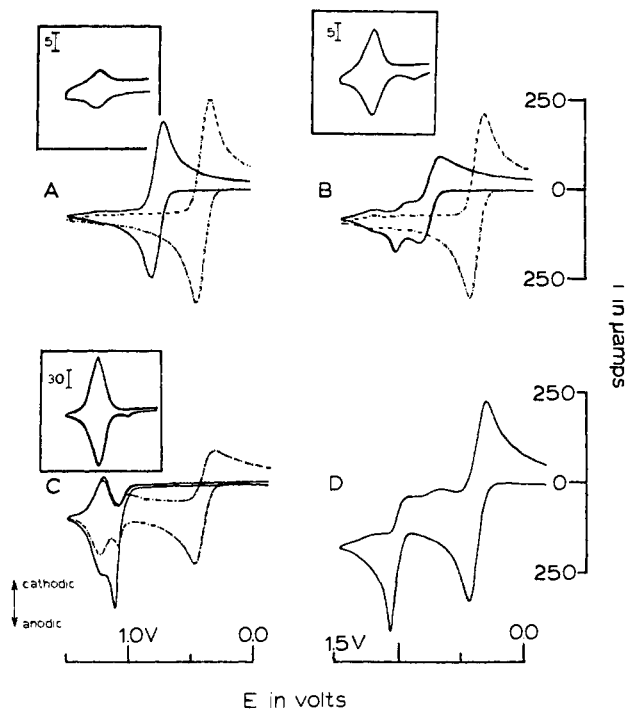


**Figure 2.** Cyclic voltammograms of Fe( $\eta^5$ -C<sub>5</sub>H<sub>5</sub>)<sub>2</sub> (solid line;  $5.1 \times 10^{-3}$  M) and Ru(bpy)<sub>2</sub>(py)Cl<sup>+</sup> (dashed line;  $5.1 \times 10^{-3}$  M) at a platinum electrode coated with varying amounts of electropolymerized Ru(bpy)<sub>2</sub>(vpy)<sub>2</sub><sup>2+</sup>. The insets show cyclic voltammograms of the coated electrode without added complex. The current scales are shown as insets in  $\mu$ amps. Coverages are: A,  $2.4 \times 10^{-10}$  mol/cm<sup>2</sup> (ca. 3 monolayers);<sup>7</sup> B,  $9.9 \times 10^{-10}$  mol/cm<sup>2</sup> (ca. 10 monolayers);<sup>7</sup> C,  $5.2 \times 10^{-9}$  mol/cm<sup>2</sup> (ca. 54 monolayers).<sup>7</sup> Figure D shows a cyclic voltammogram of a mixture of Fe( $\eta^5$ -C<sub>5</sub>H<sub>5</sub>)<sub>2</sub> ( $5.2 \times 10^{-3}$  M) and Ru(bpy)<sub>2</sub>(py)Cl<sup>+</sup> ( $5.2 \times 10^{-3}$  M) at the same polymer surface coverage shown in B. The scan rate is 200 mV/s.

(III)/Ru(II) wave ( $E_{1/2} = 1.23$  V) and bpy<sup>0/-2-</sup> waves ( $E_{1/2} = -1.33, -1.53$  V), there appear oxidative and reductive prewaves, as was first noted by Abruña.<sup>3</sup> We have observed the properties of these prewaves under a variety of conditions and their possible origins will be presented in a later publication. For now it is sufficient to note that the peak potentials and peak currents increase with increasing surface coverage. In addition, the peak currents decrease to a steady-state level with repeated scanning, but can be regenerated by scanning through the potential region for the opposite prewave (note Figure 1).

However, the point to be addressed in this manuscript is the ability of the polymer film to act as a mediator between the electrode and the external solution. The results of an experiment which probes this behavior are shown in Figure 2. The cyclic voltammograms of acetonitrile solutions of [Ru(bpy)<sub>2</sub>(py)Cl](PF<sub>6</sub>) and Fe( $\eta^5$ -C<sub>5</sub>H<sub>5</sub>)<sub>2</sub> were made with an electrode covered with increasingly thicker films of Ru(bpy)<sub>2</sub>(vpy)<sub>2</sub><sup>2+</sup>. Under the same conditions but at bare electrodes, potentials for the Ru(bpy)<sub>2</sub>(py)Cl<sup>2+/+</sup> and Fe( $\eta^5$ -C<sub>5</sub>H<sub>5</sub>)<sub>2</sub><sup>+0</sup> couples are 0.79 and 0.40 V, respectively. As shown in Figure 2A (low surface coverage), the

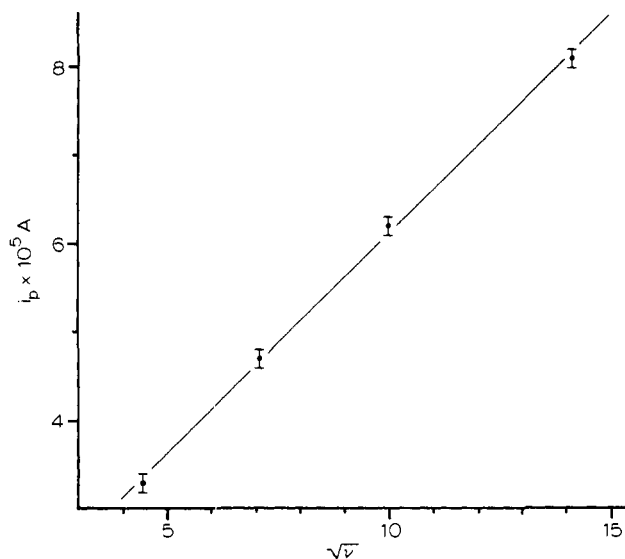


**Figure 3.** Plot of  $i_{\text{peak}}$  for the diffusional wave of Ru(bpy)<sub>2</sub>(py)Cl<sup>+</sup> ( $4.6 \times 10^{-3}$  M) vs. (scan rate)<sup>1/2</sup> at a platinum electrode coated with  $3 \times 10^{-10}$  mol/cm<sup>2</sup> (ca. 3 monolayers) of poly-Ru(bpy)<sub>2</sub>(vpy)<sub>2</sub><sup>2+</sup>.

wave shapes for both of the solution species, Ru(bpy)<sub>2</sub>(py)Cl<sup>+</sup> and Fe( $\eta^5$ -C<sub>5</sub>H<sub>5</sub>)<sub>2</sub>, are diffusional in character. The diffusional nature of the waves is suggested in Figure 3 where a linear dependence between peak current ( $i_p$ ) and the square root of the sweep rate ( $\nu^{1/2}$ ) is shown to exist for the [Ru(bpy)<sub>2</sub>(py)Cl]<sup>2+/+</sup> couple. Note, however, that extrapolation of the plot does not yield a zero intercept as should be the case for ideal behavior. A possible cause of this non-ideality is entrapment of the solution couple at the electrode by the polymer film, but additional experimental results are clearly needed.

The data in Figure 2A were obtained at a relatively thin film (ca. 3 layers) where the method used for estimating surface coverage was discussed in the Experimental Section. It should be noted here as well that it is doubtful that the polymeric "film" grows in regular layers and, as a consequence, several "layers" may be required to achieve complete coverage of the surface.

As the surface coverage is increased, the peak currents for the solution species decrease, suggesting that less effective electrode area is available. If the surface coverage is increased to ca. 10 monolayers (Figure 2B), the Fe( $\eta^5$ -C<sub>5</sub>H<sub>5</sub>)<sub>2</sub><sup>+0</sup> wave remains diffusionally shaped, but the Ru(bpy)<sub>2</sub>(py)Cl<sup>2+/+</sup> wave becomes distorted. This distortion may be interpreted as the onset of membrane-controlled diffusion,<sup>10</sup> since the solution species must diffuse through holes and channels in the film to get to the electrode.

Concomitant with distortion of the wave at the  $E_{1/2}$  of the Ru(bpy)<sub>2</sub>(py)Cl<sup>2+/+</sup> couple is the advent of an oxidative spike which occurs at a potential between the oxidative prewave and the Ru(II)/Ru(III) oxidation of the surface-bound polymer. Preliminary results indicate that the oxidative prewave triggers the spike, and this observation will be explored in a later publication. The peak current of the spike,  $i_p$ , is proportional to the bulk concentration of Ru(bpy)<sub>2</sub>(py)Cl<sup>+</sup> and varies linearly with  $\nu^{1/2}$  as shown in Figures 4 and 5, respectively. Moreover, extrapolation of the plot in Figure 5 yields a zero intercept. These observations suggest the importance of diffusion of the substrate to the film in the film-mediated oxidation of the solution couple.

Figure 6 shows that at slower scan rates the diffusional wave assumes a more nearly ideal wave shape and increases in peak current at the expense of the spike. The observations summarized

(10) Murray, R. W., Ph.D. Dissertation, Northwestern University, Evanston, IL, 1966.

(11) A referee has suggested that if a sufficiently fast sweep rate was used, the ferrocene<sup>+0</sup> reduction wave should be larger than the ferrocene<sup>0/+</sup> oxidation wave because of ferrocene catalysis of the reduction of [Ru<sup>III</sup>(bpy)<sub>2</sub>(py)Cl]<sup>2+</sup> still at or near the electrode. We have not observed this effect at our scan rates, but it is a point that will be investigated in the future.

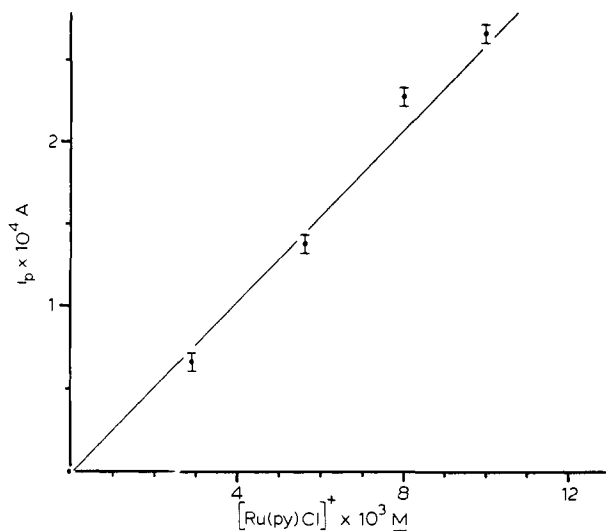


**Figure 4.** Plot of  $i_p$  spike vs. the concentration of  $Ru(bpy)_2(py)Cl^+$  platinum electrode coated with  $1.5 \times 10^{-9}$  mol/cm<sup>2</sup> (ca. 15 monolayers) of poly- $Ru(bpy)_2(vpy)_2^{2+}$ . The scan rate is 200 mV/s.

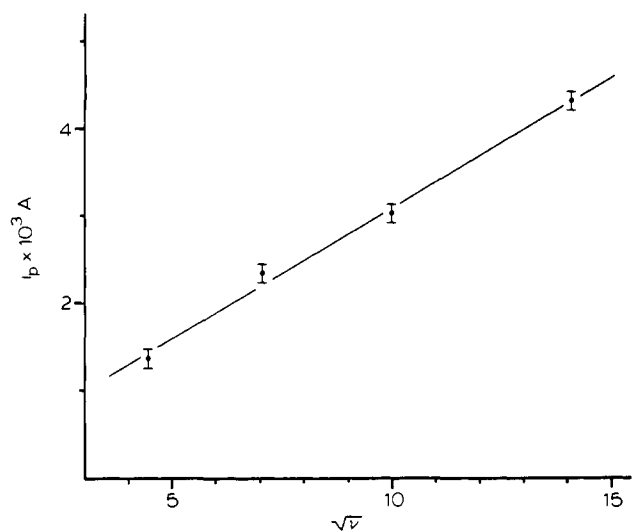


**Figure 5.** Plot of  $i_p$  spike vs.  $(\text{scan rate})^{1/2}$  for the film-mediated oxidation of  $Ru(bpy)_2(py)Cl^+$  (ca.  $5 \times 10^{-3}$  M) at a platinum electrode coated with  $5.8 \times 10^{-9}$  mol/cm<sup>2</sup> (ca. 60 monolayers) of poly- $Ru(bpy)_2(vpy)_2^{2+}$ .

in Figure 6 are important since they demonstrate a frequency (scan rate) dependence in the current-potential characteristics of the films as mediators. The series of experiments also clearly demonstrate the existence of two discrete pathways for net charge transfer—a diffusional or mass-transfer pathway which is a slow process at thick films (at least on the time scale of cyclic voltammetry) and a charge-transfer pathway which is dictated by the redox properties of the film. The wave for the  $Fe(\eta^5-C_5H_5)_2^{+/0}$  couple undergoes qualitatively similar changes in electrochemical behavior, but the appearance of an oxidative spike requires considerably higher surface coverages as shown in Figure 2C.

One interesting carry-over from the surface-coverage dependencies in Figure 2A–C is a basis for obtaining the selective oxidation of  $Fe(\eta^5-C_5H_5)_2$  in the presence of  $[Ru(bpy)_2(py)Cl]^+$ . The selectivity is possible even though both couples involved are essentially electrochemically reversible at nonpolymer-coated electrodes. The point is demonstrated in Figure 2D which, as for Figure 2B, is carried out at a film of intermediate thickness (ca. 10 monolayers). The only difference between the experiments shown in Figure 2B and Figure 2D is that in the latter, both  $Fe(\eta^5-C_5H_5)_2$  and  $[Ru(bpy)_2(py)Cl]^+$  are present in the external solution simultaneously. In comparing the two experiments, the striking point to note is that when both ferrocene and the ruthenium complex are present, an oxidative scan through the po-

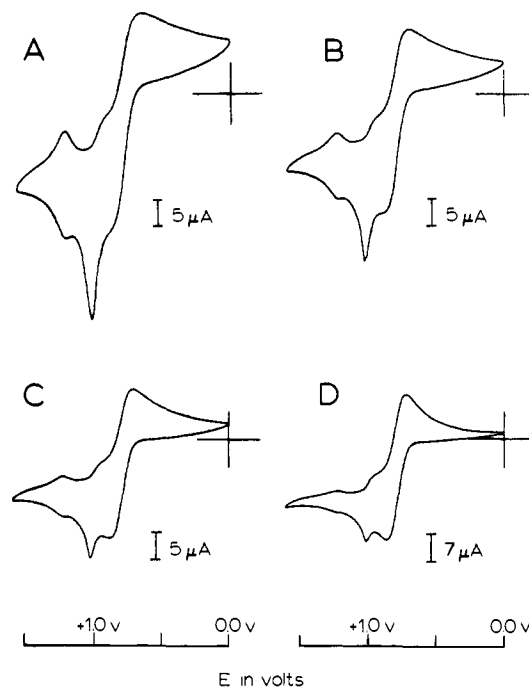


**Figure 6.** Cyclic voltammograms of a  $2.4 \times 10^{-3}$  M solution of  $Ru(bpy)_2(py)Cl^+$  at a platinum electrode coated with  $6.8 \times 10^{-10}$  mol/cm<sup>2</sup> (ca. 7 monolayers) of poly- $Ru(bpy)_2(vpy)_2^{2+}$  at 200 mV/s (A), 100 mV/s (B), 50 mV/s (C), and 20 mV/s (D). It should be noted that the apparent reversal in peak potentials for the anodic and cathodic components of the surface wave ( $E_p$  for the anodic wave occurs at a potential negative of  $E_p$  for the cathodic wave) is an artifact. The artifact is caused by a distortion of the normal wave shape due to the close proximity of the oxidative spike.

tential region (0.3–0.8 V) where both of the couples undergo oxidation shows a diffusional wave only for the oxidation of  $Fe(\eta^5-C_5H_5)_2$ . By comparing Figures 2B and 2D, it is apparent that with ferrocene added the diffusional pathway for the  $[Ru(bpy)_2(py)Cl]^{2+/+}$  couple is completely blocked. Under these conditions, oxidation of  $Ru(bpy)_2(py)Cl^+$  occurs solely by the external or charge-transfer pathway characterized by the oxidative spike. Although it is a point which needs exploring in more detail, it seems inescapable that the basis for selectivity at the coated electrodes lies in the relative permeability and diffusional characteristics of the redox reagents within the polymer film.

At thick films, (Figure 2C; ca. 54 monolayers) the charge-transport pathway represented by the spike provides the sole mechanism for oxidation of  $Ru^{II}(bpy)_2(py)Cl^+$ . In contrast to the diffusional pathway where both oxidative and reductive components of the voltammetric wave are observed, *this pathway involves a directed electron transfer to the electrode*. There is no reverse charge transfer component analogue of the oxidative spike, at least on the time scale of the experiment. At thick films, oxidation of the external couple occurs by charge transfer through the films rather than by mass transfer (diffusion). Reduction of  $Ru^{III}(bpy)_2(py)Cl^{2+}$  can occur, but only at very negative potentials. When the cathodic prewave at  $E \leq -1.1$  V is reached (note Figure 1), reduction can occur, but now it is via a reductive spike as shown in Figure 7C. It should be pointed out that in Figure 7C, the following reductive waves can be seen in passing from positive to negative potentials:  $Ru(III)/Ru(II)$  (surface couple), reductive spike,  $bpy^{0/-}$  (surface couple),  $bpy^{0/-}$  (solution couple), and  $bpy^{2-/1-}$  (solution couple). The second  $bpy$  reduction for the surface couple is lost beneath the two  $bpy$  reductions of the solution couple. In Figure 7, voltammograms for a modified electrode and for  $[Ru(bpy)_2(py)Cl](PF_6)$  at an unmodified electrode are shown for reference.

## Discussion

As in the bilayer experiment reported earlier,<sup>1</sup> directed charge transfer in the films has its origin in the potential differences

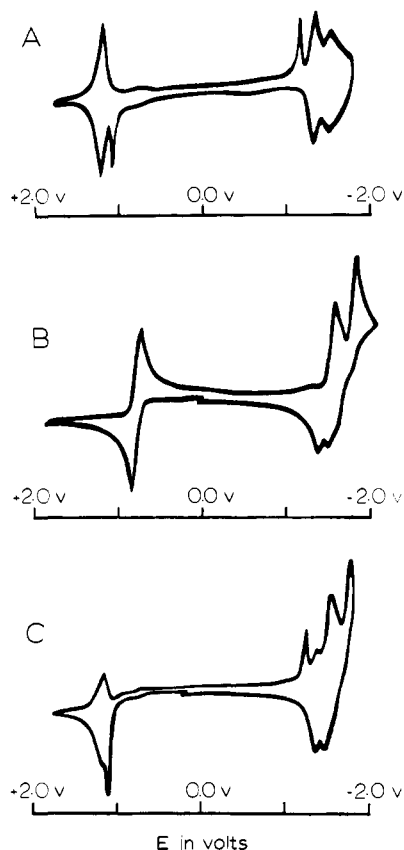
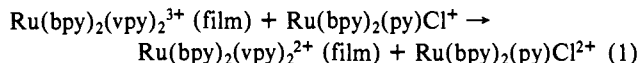


**Figure 7.** Cyclic voltammograms of: (A) a platinum electrode coated with poly-Ru(bpy)<sub>2</sub>(vpy)<sub>2</sub><sup>2+</sup>; (B) Ru(bpy)<sub>2</sub>(py)Cl<sup>+</sup> at a bare platinum electrode; and (C) the solution in B measured with the modified electrode in A. Recorded on a Tektronix 564B storage oscilloscope. Note that the current scale in A is not the same as in B and C.

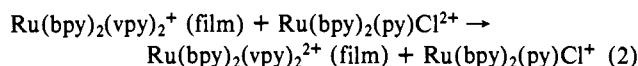
between the redox couples adjacent to and remote from the electrode surface. If diffusion through the film is slow on the time scale of the experiment, oxidation of the external couple is restricted to the charge-transfer pathway through the film. Oxidation by this pathway cannot occur until the potential for the film couple is approached. Partial oxidation of Ru(II) to Ru(III) within the film leads to a mixed-valence polymer which creates a pathway for charge transfer through the film by electron hopping. From electron-transfer experiments on related chemical materials, it is anticipated that the vibrational barrier to electron transfer within the film is relatively low.<sup>12,13</sup> It should also be

noted that there is a substantial driving force favoring charge transfer by this pathway since the reaction in eq 1 is favored by 0.46 V. In the absence of a diffusional pathway, re-reduction



of Ru(bpy)<sub>2</sub>(py)Cl<sup>2+</sup> is necessarily slow because charge transfer through the film must occur by the reverse of eq 1 which is disfavored by 0.46 V. The origin of the directed charge transfer has its basis in the same principle involved in the redox potential "cascade" effect found in membrane-based, directed charge transfer in mitochondria.

Re-reduction of Ru(bpy)<sub>2</sub>(py)Cl<sup>2+</sup> can occur by electron transfer hopping from the electrode through the film but only at very negative potentials. At negative potentials reduction occurs at π\* (bpy) levels in the films and re-reduction by electron hopping is favored by ca. 2.0 V (eq 2).



The net effect of the film-mediated redox process at thick films is to convert a chemically and electrochemically reversible couple with  $\Delta E_p = |E_p(\text{oxidation}) - E_p(\text{reduction})| \approx 60 \text{ mV}$  into a chemically reversible but charge-transfer highly-irreversible couple ( $\Delta E_p \approx 2 \text{ V}$ ) at the electrode. The point is, of course, that the oxidation/reduction potentials observed at the electrode are now dictated by the characteristics of the film rather than by the inherent properties of the redox couple.

The observations made here show that there are two discrete pathways for charge transfer through the electropolymerized films. The diffusional pathway provides a basis for selectivity between reagents in the external solution. The existence of the charge-transfer or electron-hopping pathway observed here and earlier with bilayers<sup>1,3</sup> shows that metallopolymer films have intrinsic characteristics which could lead to materials having properties usually associated with solid-state electronic devices such as diodes and transistors. In terms of possible photochemical energy conversion schemes, the observations of directed charge transfer and selectivity begin to show how to transfer the rectifying properties observed upon photolysis at a semiconductor-solution interface<sup>14-17</sup> to any electrode material.

**Acknowledgement** is made to the Army Research Office-Durham under contract No. DAAG29-79-C-0044 for support of this research.

(14) Gerisher, H. In "Physical Chemistry—An Advanced Treatise", Eyring, H., Henderson, D., Jost, W., Eds.; Academic Press: New York; Vol. 9A, pp 463-542.

(15) Heller, A., Ed. "Semiconductor Liquid-Junction Solar Cells", Proceedings of the Electrochemical Society 1977, 77-3.

(16) Wrighton, M. *Acc. Chem. Res.* **1979**, *12*, 303.

(17) Nozik, A. *Annu. Rev. Phys. Chem.* **1978**, *29*, 189.

(12) Meyer, T. J. *Acc. Chem. Res.* **1978**, *11*, 94.

(13) Powers, M. J.; Meyer, T. J. *J. Am. Chem. Soc.*, **1980**, *102*, 1289-1297.